

Primary beam for AARTFAAC-6 based on simulations

Peeyush Prasad, Michel Arts

September 4, 2015

1 Introduction

The purpose of this document is to generate a reliable primary beam model for AARTFAAC-6. This is necessary to compensate for the primary beam response in all-sky images, whose effect is to attenuate sources away from the pointing center. The AARTFAAC system piggybacks on the LOFAR antennae in 12 stations including the 6 superterp stations and the first ring of station surrounding it. The LOFAR antennae come in two varieties:

- The Low Band Antenna (LBA), consisting of a pair of crossed inverted-V dipoles and a ground plane. 96 such antennas are present in a station. However, only a subset of 48 can be used at a time due to restrictions in receiver hardware at the Dutch stations. Note that when 48 antennas are used, the remaining 48 are turned off, i.e., their LNAs are not biased, and hence present a different input impedance compared to when the LNAs are biased. This subset can be one of LBA_OUTER (outer 48) and LBA_INNER (inner 48) antennas.
- The High Band Antenna (HBA), consisting of a pair of crossed bow-tie elements as the basic unit. The HBA antennas are arranged in a 4x4 square array (a tile), and their analog beamformed output is the primary output available for further processing. 48 tiles are arranged per station into two dense fields of 24 tiles each. Depending on the station configuration, either one or both fields can be used. The LBAs and the unused HBA tiles are all turned off when LOFAR is in HBA mode.

Several attempts have been already made to model the antenna response ([1], [2]) and reconcile them with observations (usually illuminating the antenna under test with a calibrated source in its far field). These have typically looked at a single antenna in isolation, while we look at the full array of 576 antennas in the superterp, in the available configurations.

2 Simulations

The entire AARTFAAC-6 station LBA system has been electromagnetically simulated using WIPL-D. Each dipole of every antenna has accurate placement, orientation (for polarization) and dimensional information, along with a reasonable value for the soil permittivity and conductivity. Further, a finite ground plane per antenna has been simulated (instead of the infinite plane assumption). This simulation is available at `prasad@dop312: /WORK/AARTFAAC/Afaac_matlab_calib/LBA_beam/arts_sim/LBA_core.mat`. A simulation with a finer, 1MHz frequency grid between 40-60 MHz is available in the file `LBA_core_fine.mat`.

2.1 Underlying theory

A radiator can emit electromagnetic radiation with various states of polarization. In an orthonormal coordinate system with z-axis along the direction of propagation, a quasi-monochromatically emitted vector electromagnetic field \mathbf{e} can be represented by a column vector of 2 complex numbers, $[e_\theta e_\phi]$, with each being a component orthogonal to the direction of propagation. A particular state of polarized emission can be described by the emission stokes parameters, which are designated by I_E, Q_E, U_E, V_E , with I being total

intensity, Q and U being the fraction of linear polarization and V being the fraction of circular polarization in the emission. The equivalent stokes description of the emitter in terms of its vector components are:

$$\begin{aligned} I_E &= \langle e_\theta \cdot e_\theta^* \rangle + \langle e_\phi \cdot e_\phi^* \rangle \\ Q_E &= \langle e_\theta \cdot e_\theta^* \rangle - \langle e_\phi \cdot e_\phi^* \rangle \\ U_E &= \langle e_\theta \cdot e_\phi^* \rangle + \langle e_\phi \cdot e_\theta^* \rangle \\ jV_E &= \langle e_\theta \cdot e_\phi^* \rangle - \langle e_\phi \cdot e_\theta^* \rangle \end{aligned} \quad (1)$$

The stokes parameters of the emission are related to the emission vector via the emitter's coherency matrix, defined to be $\mathbf{E}_{\theta\phi} = \mathbf{e} \cdot \mathbf{e}^H$:

$$\mathbf{E}_{\theta\phi} = 0.5 \begin{bmatrix} I_E + Q_E & U_E + jV_E \\ U_E - jV_E & I_E - Q_E \end{bmatrix} \quad (2)$$

The receiving antenna usually consists of orthogonally aligned receiving elements, here designated as having \mathbf{x} and \mathbf{y} components/dipoles. Depending on the type and other parameters of the receiver, it has its own state of polarization, designated by I_V, Q_V, U_V, V_V . This state of the antenna polarization determines the sensitivity of the antenna to emission of a particular polarization state. The simulation aims to provide a complete description of the antenna response to all states of polarized emission. This is achieved by carrying out the simulation using an orthogonal component of the emitter one at a time. Any desired emission polarization state can be generated via suitable manipulation of the emitters' coherency matrix, $E_{\theta\phi} = e \cdot e^H$, shown above. For specifying the emission as unpolarized ($I=1, Q=U=V=0$), the coherency matrix is:

$$\begin{bmatrix} 1 & 0 \\ 0 & 1 \end{bmatrix} \quad (3)$$

while for linearly polarized emission ($I=1, Q=1, U=V=0$), the emitter's coherency matrix is

$$\begin{bmatrix} 1 & 0 \\ 0 & 0 \end{bmatrix} \quad (4)$$

These can be derived from equation 1.

Note that a complete representation of both the transmitted electromagnetic field, as well as the received voltages at the antenna requires a stokes representation in **each** case.

A model of the dipole interfaced with the LNA is shown in Fig. 1. The LNA impedance is modeled by the RC circuit with R and C in parallel, as shown. The antenna impedance includes the effect of mutual coupling, and is generated by the simulation. The LNA impedance is computed with the the equations in Fig. 2.

2.2 LNA impedance

A change in the impedance of the LNA affects the resonance frequency of the front-end response. In these studies, two different values of the impedance have been used, one using the actual values of the R and C used in the implemented LNA circuit, while the other are fits to measurements using the LNA model as shown in Fig. 1.

- The LNA schematic shows an R and C in series, with values $R = 36\Omega$, $C = 4.2 \text{ pF}$ (TODO: reference to front-end schematics).
- The emperical R and C values are derived by fitting a simulated beamshape (after optimization of the R and C values), to the measured beamshape. These latter values are available from [1] pg. 47, with values of $R = 700\Omega$ and $C = 15\text{pF}$. The simulations of the beam shape have been carried out using both these values, and a comparison has been made in section 4.

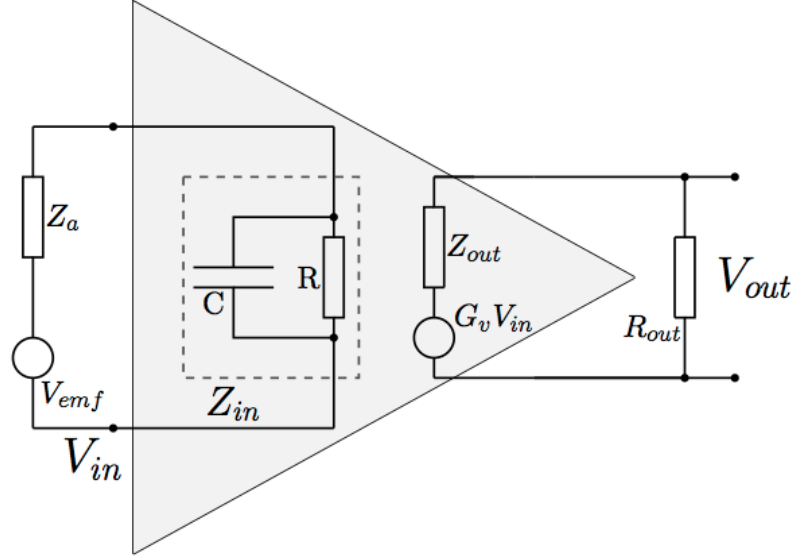


Figure 4.3: Equivalent circuit of the LBA. The circuit represents a voltage source including an internal resistance which is equal to the antenna impedance. The LNA, which works as an operational amplifier, is located directly behind the antenna. It consists of a capacitor C and a resistor R . The output resistor R_{out} has to be matched to the impedance of the LNA, Z_{out} .

Figure 1: The LNA model interfaced with the dipole, for LBA antennas. From [1]

$$\frac{V_{out}}{V_{emf}} = G_V \cdot \frac{Z_{in}}{Z_{in} + Z_a} \cdot \frac{R_{out}}{R_{out} + Z_{out}} \quad (4.18)$$

$$Z_{in} = \frac{R}{1 + j\omega RC}, \quad (4.19)$$

Figure 2: The LNA impedance calculation. From [1]

2.3 Mutual coupling

The close proximity of the antennas in the cluster results in reflections off individual elements being received by neighbouring ones. The effect of this is to distort the resulting beam shape. Individual antennas whose LNAs are turned off present a different input impedance, and can thus affect the mutual coupling. In the LOFAR core, only the subset of 48 antennas being beamformed (LBA.OUTER and LBA.INNER configurations) are turned on. The resulting changed impedance of the remaining (unbiased) antennas might affect the beamshape. This is incorporated in the simulations, which proceed by turning off the response of all other dipoles except the one under test. Subsequently, the different array configurations can be mimicked by creating a subset of the relevant dipoles. In the HBA, all tiles within a ear are turned on for the more popular configurations, and hence the mutual coupling effects are expected to remain the same across array configurations. Mutual coupling effects have been incorporated into the simulations, resulting in the embedded beam patterns for individual dipoles of all antennas being available between 10-90 MHz.

2.4 Simulation products

The simulations are carried over a grid of directions and frequencies. At every chosen direction, the polarized point source is placed at infinity, resulting in a polarized plane wave impinging on the array. The simulation has a 5 MHz spectral spacing and a 5degx5deg spatial grid. The details of the individual antennas and the simulation in general are available in [3].

The simulation products consist of the embedded element patterns of the individual dipoles, and not the array pattern. This implies that different antennas are not phased up towards the source of emission, resulting in a phase difference due to propagation delay between them. The array response towards any direction can be obtained via beamforming in that direction.

The simulation produces:

- **g.z:** Open circuit voltages as a function of direction, frequency, antenna polarization and electric field component. This is the voltage induced in the antenna dipoles by the incoming EM wave alone, and does not include any downstream component like the LNA etc.
- **Zant:** The impedance matrix of the dipole array, as a function of freq. This includes the mutual coupling effect due to the reflections off nearby antennae.
- **Positions:** The positions of the dipoles, referred to the first dipole. There are 96 antennas * 2 pols/ant * 6 stations = 1152 dipoles. The inner antennas (LBA.INNER) of all stations occupy the first 576 locations, while the outer antennas (LBA.OUTER) occupy the remaining 576 locations in this matrix. The same order is maintained in the open circuit voltage products.
- **Theta,Phi:** The direction grid for which the simulation has been carried out, and the beam pattern sampled.
- **Freq:** The frequencies at which the simulation is carried out, 5MHz spacing between 10-90 MHz for LBA.

2.5 Generating the beam pattern

We are interested in obtaining the beam pattern for each **antenna** stokes parameter. The voltage v_x and v_y induced at the output of each polarized dipole making up the antenna is modulated by the gain (beam pattern) of the antenna. The gain is a combination of the open circuit voltage and the nett. impedance, and can be modeled as:

$$\begin{bmatrix} v_x \\ v_y \end{bmatrix} = \begin{bmatrix} g_{x,\theta} & g_{x,\phi} \\ g_{y,\theta} & g_{y,\phi} \end{bmatrix} \times \begin{bmatrix} e_\theta \\ e_\phi \end{bmatrix} \quad (5)$$

or,

$$\mathbf{v} = \mathbf{G}\mathbf{e} \quad (6)$$

The coherency matrix of dipole voltages

$$\mathbf{V}_{\mathbf{xy}} = \mathbf{v}\mathbf{v}^H = \begin{bmatrix} v_x v_x^* & v_x v_y^* \\ v_y v_x^* & v_y v_y^* \end{bmatrix} \quad (7)$$

can be written as

$$\mathbf{V}_{\mathbf{xy}} = \mathbf{G}\mathbf{E}_{\theta\phi}\mathbf{G}^H \quad (8)$$

where \mathbf{G} is the gain matrix and $\mathbf{E}_{\theta\phi} = \mathbf{e}\mathbf{e}^H$ is the coherency matrix of the incoming electric field. Once the dipole voltage coherency matrix is known, the stokes parametres can be obtained from it by:

$$\begin{aligned} I_v &= \langle v_x v_x^* \rangle + \langle v_y v_y^* \rangle \\ Q_v &= \langle v_x v_x^* \rangle - \langle v_y v_y^* \rangle \\ U_v &= \langle v_x v_y^* \rangle + \langle v_y v_x^* \rangle \\ jV_v &= \langle v_x v_y^* \rangle - \langle v_y v_x^* \rangle \end{aligned} \quad (9)$$

The model of the analog receiver system is illustrated in [1], and is a simple LNA in series with the antenna. We assume the voltage gain of the LNAs as unity. This results in the beam patterns begin a scale factor away from the actual gain, but does not affect the pattern spatial characteristics.

The gain of the system is then determined using the antenna impedance provided by the simulation and the gain and impedance of a dipole. The output voltage after the LNA can then be determined by multiplying the open circuit voltage of a dipole with its gain. Effectively, this is the same as multiplying the gain matrix \mathbf{G} of the antenna with the gain of the LNA and using this new gain matrix to calculate the coherency matrix \mathbf{V}_{xy} . This voltage coherency matrix is used to determine the Stokes-I beam.

The relevant matlab script to generate the stoke-I beams is the matlab class implementation SimElementBeam.m in the Afaac_matlab.calib/ folder. Its example usage is provided in the header comment, and consists of creating an object of type SimElementBeam with an array configuration and LBA/HBA bool. Then, the tasks createAvgBeam() and genPlots() can be used to generate and plot the beam parameters in l,m coordinates.

3 Results: LBA with LNA as series RC circuit with schematic values

The presented results are stokes-I beams organized as a function of frequency, array configuration, station, and presented in l,m coordinates. The beam pattern is normalized to be 1 at its peak. The contours are at 75, 50 and 25 percent of the peak of the beam pattern, and are useful to show the variation of the beam pattern of stations in different array configurations due to mutual coupling. The stokes-I beam patterns of individual antenna elements, along with the location of that antenna and the cumulative average station beam pattern is available in movies (LBA_OUTER.stokesI.beam.pattern.25000000.000000MHz.avi) etc. for both configurations.

NOTE that these results have been generated using the actual values of the R and C in the frontend circuit schematics.

We first present the averaged beam pattern over all 6 superterp stations, as a function of frequency in Fig. 3, Fig. 4, Fig. 5, Fig. 6. The beam patterns are available as a zenith projection in l,m coordinates. An astronomical image generated with the same projection and size as the beam pattern matrix can be beam corrected via pixel by pixel scaling of the image pixel matrix by the beam pattern matrix. We can see that the LBA_OUTER beam patterns are quite stable till about 70MHz, and only then does the main lobe start expanding. In the LBA_INNER configuration shows a large deviation from the average beam at 25, 40MHz. This deviation is seen in every station's response, and is currently unexplained. The large variation at 70 MHz is probably due to the resonance of the dipole/LNA combine being in the vicinity.

Diameter Stokes-I average beam over 000000333333000000234307.

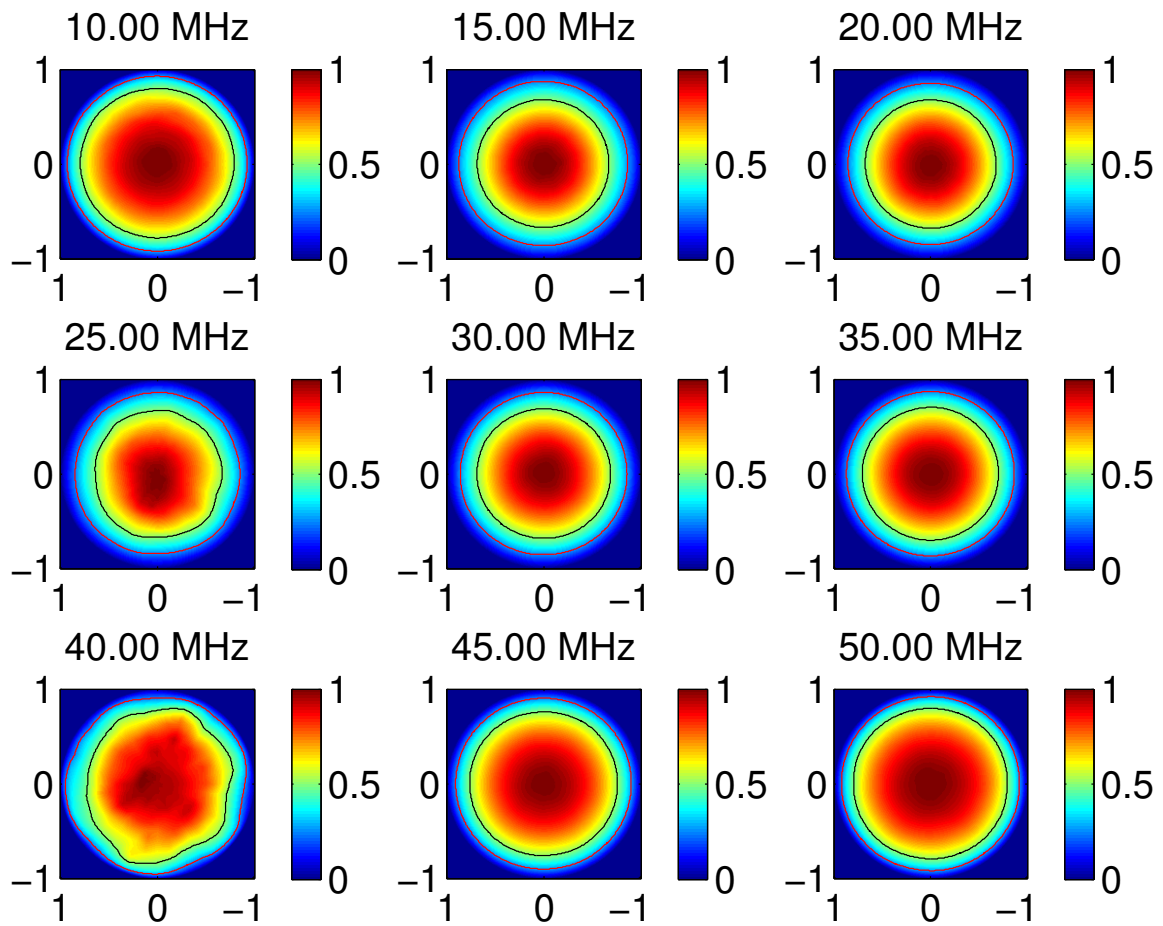


Figure 3: The spectral response of the AARTFAAC-6 average beam pattern (LBA_INNER).

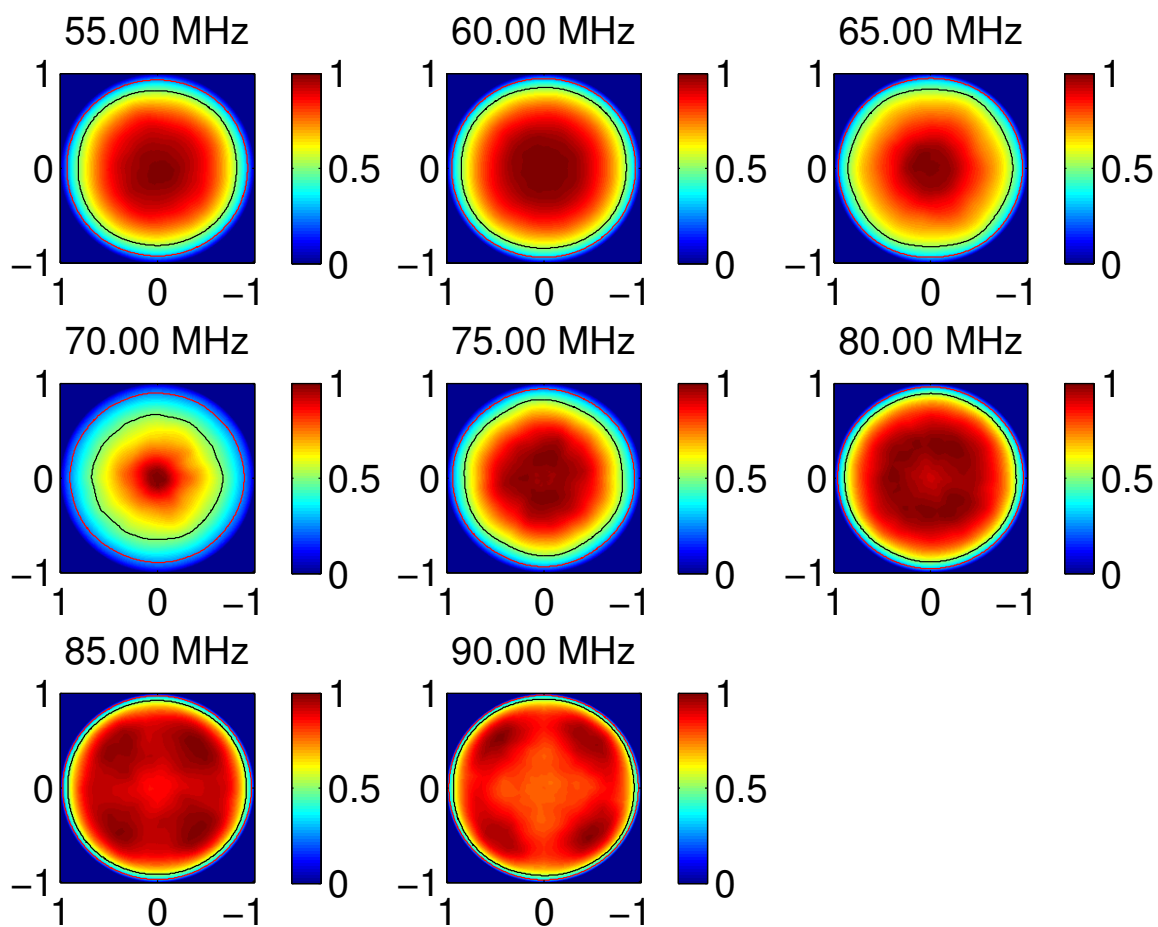
[illegible]

Figure 4: The spectral response of the AARTFAAC-6 average beam pattern (LBA_INNER).

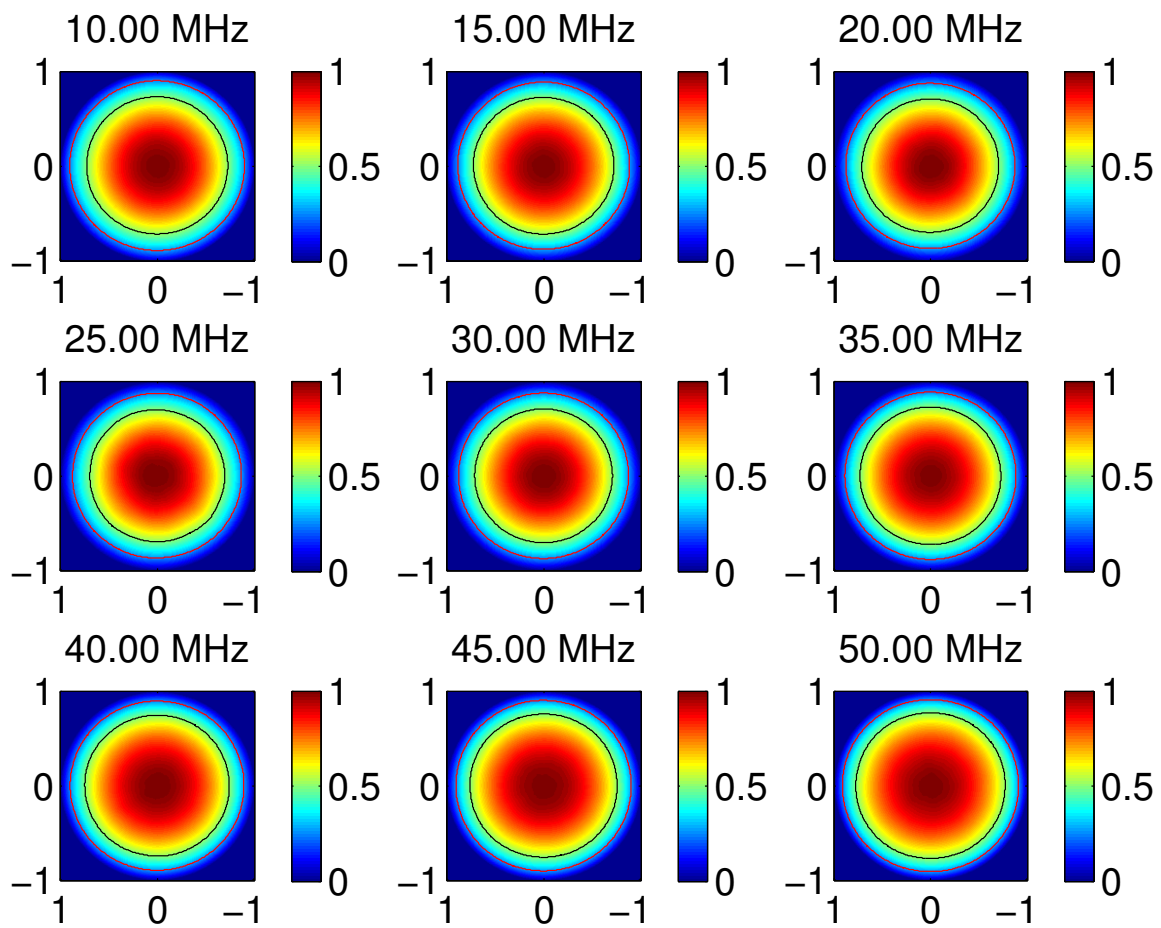
[illegible]

Figure 5: The spectral response of the AARTFAAC-6 average beam pattern (LBA-OUTER).

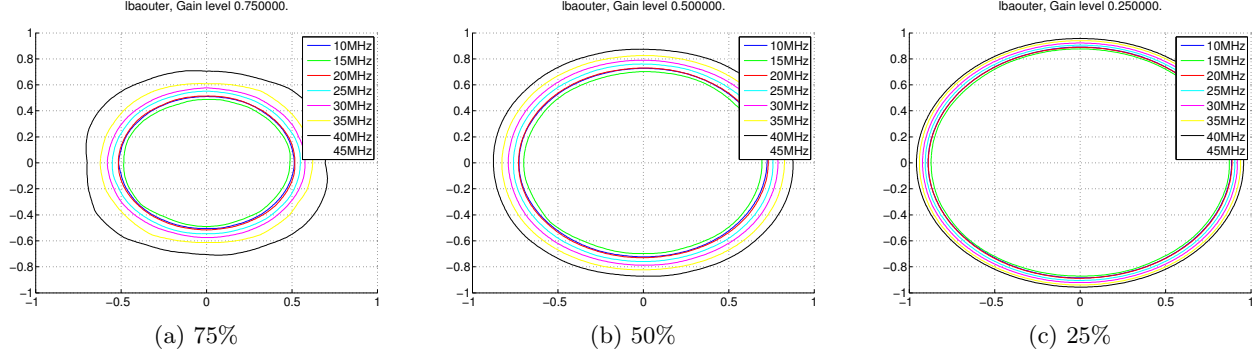


Figure 8: The spectral response of the AARTFAAC-6 average beam pattern at the 75, 50 and 25% gain contour, LBA_OUTER.

We also show the spectral response of the 1.25dB (Fig. ??,??), 3dB (Fig. ??,??), and 6dB (Fig. ??,??) average beam over the 6 superterp stations. These show the field of view of the lba_outer and inner array changing over frequency, for a fixed beam pattern contour level.

Finally, as an appendix, we present the beam patterns of individual stations, obtained by taking an average over the stokes-I beams per antenna within the station. These show the effect of mutual coupling by the drastic change in beam shape close to the LBA resonance at $\approx 55\text{MHz}$. This effect is much more pronounced in the LBA_INNER configuration (the right column). Further, CS004 shows anomolous beam patterns at 20 and 40 MHz. On examining individual antenna patterns (see movie), it is seen that a large number of antennas from this station have significantly divergent beams. The reason for this is currently unexplained.

4 Emperical Vs. circuit impedances

The commonalities between the two cases are:

- Stokes-I beamshapes of both cases show significant distortions at 25 and 40 MHz as compared to other frequencies.
- As expected due to a larger mutual coupling. the LBA_INNER configuration is much more affected by changes in impedance in both cases. The LBA_OUTER configuration does not show significant changes with changing impedance.

The following changes have been noticed after changing the LNA internal impedance to have a series representation with different R and C values:

- The resonance shifts to a higher frequency for the case of using schematic R & C values, from close to 60 MHz with emperically derived RC, to close to 70 MHz for the other case. The beampattern changes suddenly close to the resonance frequency, and this change is seen to be at 60MHz for the model LNA with emperic R and C values, while it is at 70 MHz for the series R and C values from the schematics.
- The small scale structure within the beamshape is noticably different at the higher frequencies when the two cases are compared.
- A larger spread in the 75% gain contours is seen in the case of the emperically derived values.

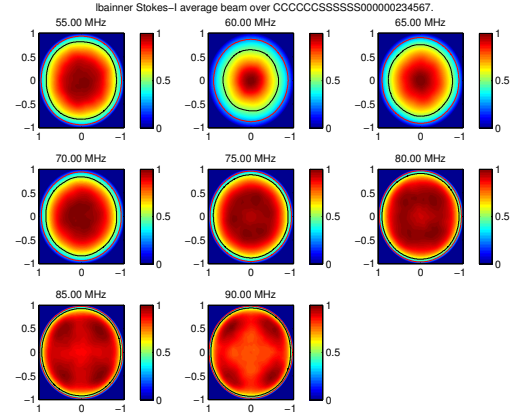
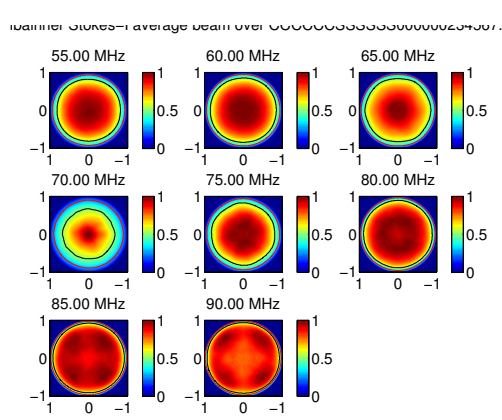
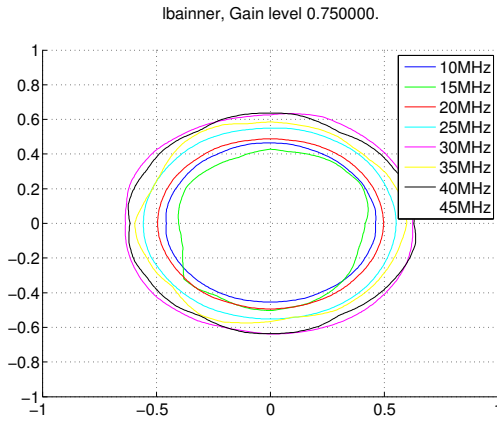
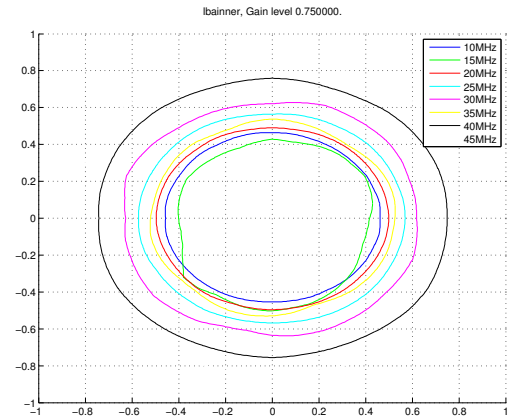


Figure 9: Average beam pattern over the superterp stations, with LNA impedance derived using empirically determined values of R & C (left) and using values from the front end schematics (right).



(a) Contours after applying the impedance based on the front-end schematics. Contours at the 75% level



(b) empirically derived R & C based gain contours at the 75% level

5 Conclusions

The simulated per dipole antenna response has been used with an empirically determined LNA impedance, as well as with the actual RC circuit in the frontend schematics to generate expected power patterns from individual stations, as well as the full superterp. The application of this model is a pixel by pixel multiplication of the pattern inverse with the generated LBA images.

The 12 station AARTFAAC is expected to be able to use the same beam patterns, due to the fact that the first ring of stations around the superterp have separations between them which are larger than the superterp. Hence, station level coupling is not expected to be a problem.

Further work would involve:

1. Confirmation of this beam model via actual observations, their correction with this beam model, and then the evaluation of their light curves for residual systematic effects. This would help choose between the LNA impedance models currently available.
2. Rescaling of the beampattern to a flux scale by either a single scale factor over the full field of view based on an astronomical source, or a scale map created by interpolation of the scale factors determined via observations of several sources.
3. The extension to AARTFAAC-6 HBA mode. This is currently not supported. Its implementation would require some beamforming of the subtile level bowtie antennas before forming the tile beams.

The following plots show the station level simulated beams using the schematic based RC values for determining the LNA impedance. The stations from left to right, top to bottom are CS002, CS003, CS004, CS005, CS006 and CS007.

References

- [1] Krause, M. M.Sc thesis
- [2] Nellis, A. Absolute flux calibration of the LOFAR LBA.
- [3] Arts, M. EM simulation of the final design of the LOFAR LBA.

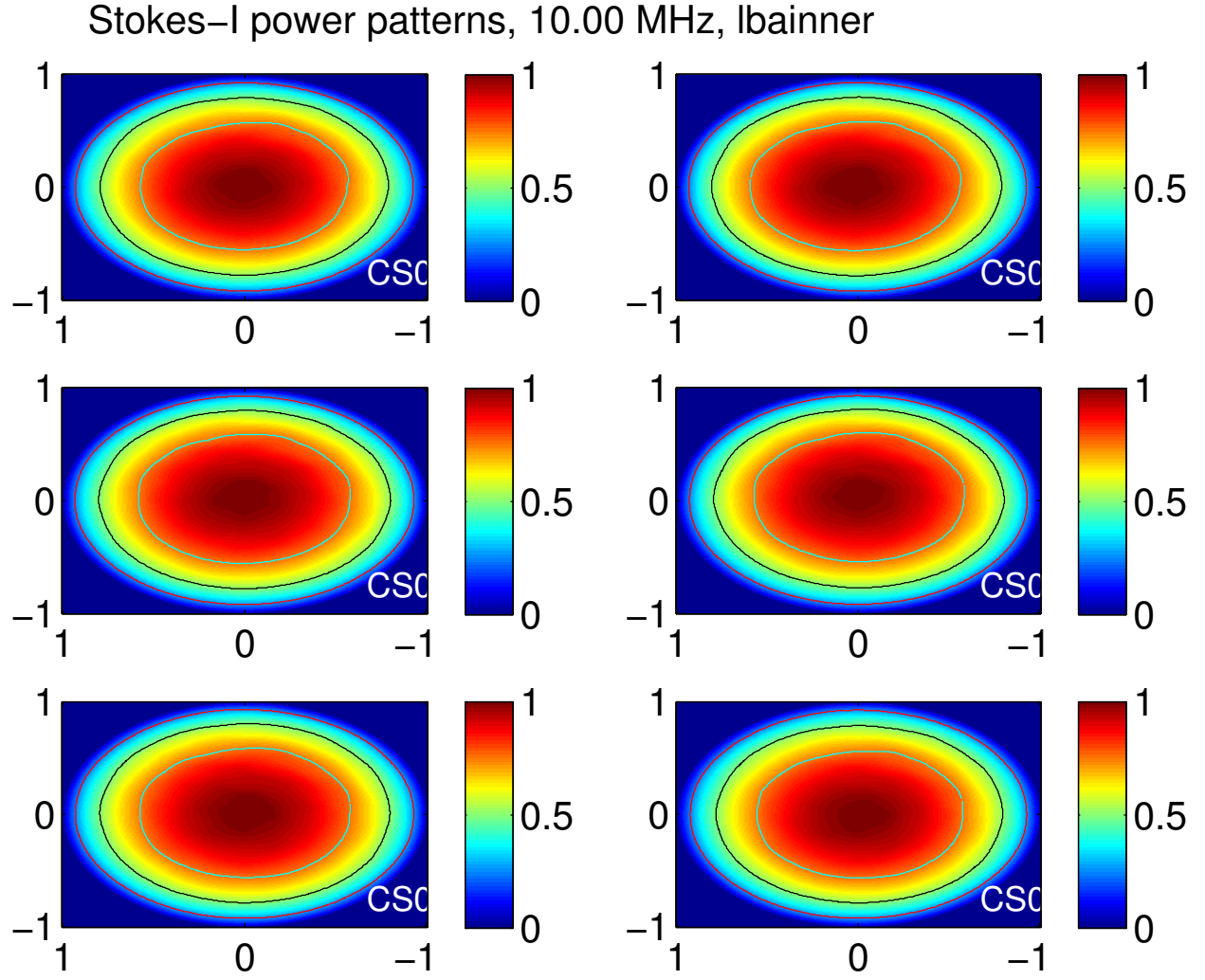


Figure 11: Stokes-I beam shapes from superterp stations for LBA INNER configuration, 10MHz.

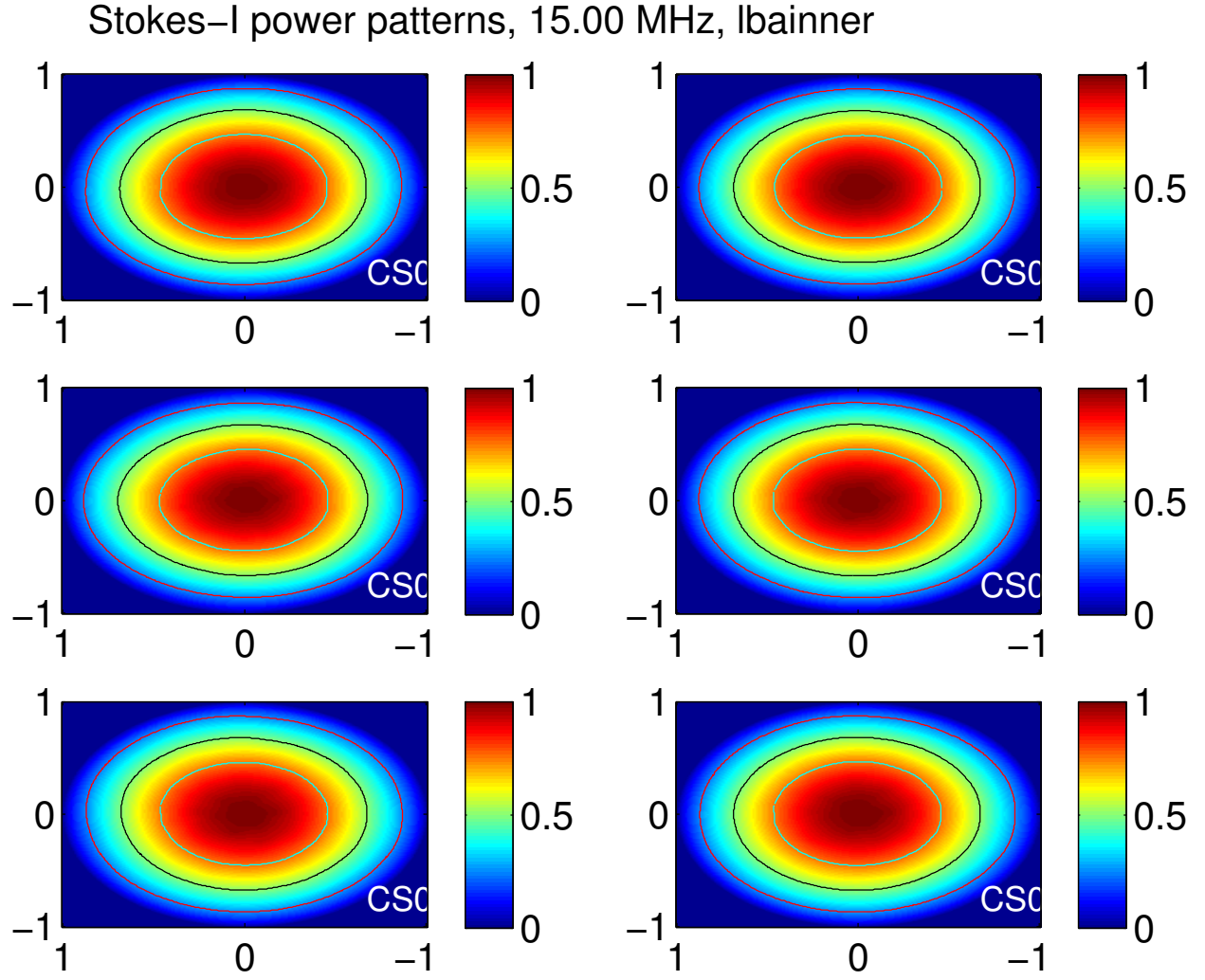


Figure 12: Stokes-I beam shapes from superterp stations for LBA INNER configuration, 15MHz.

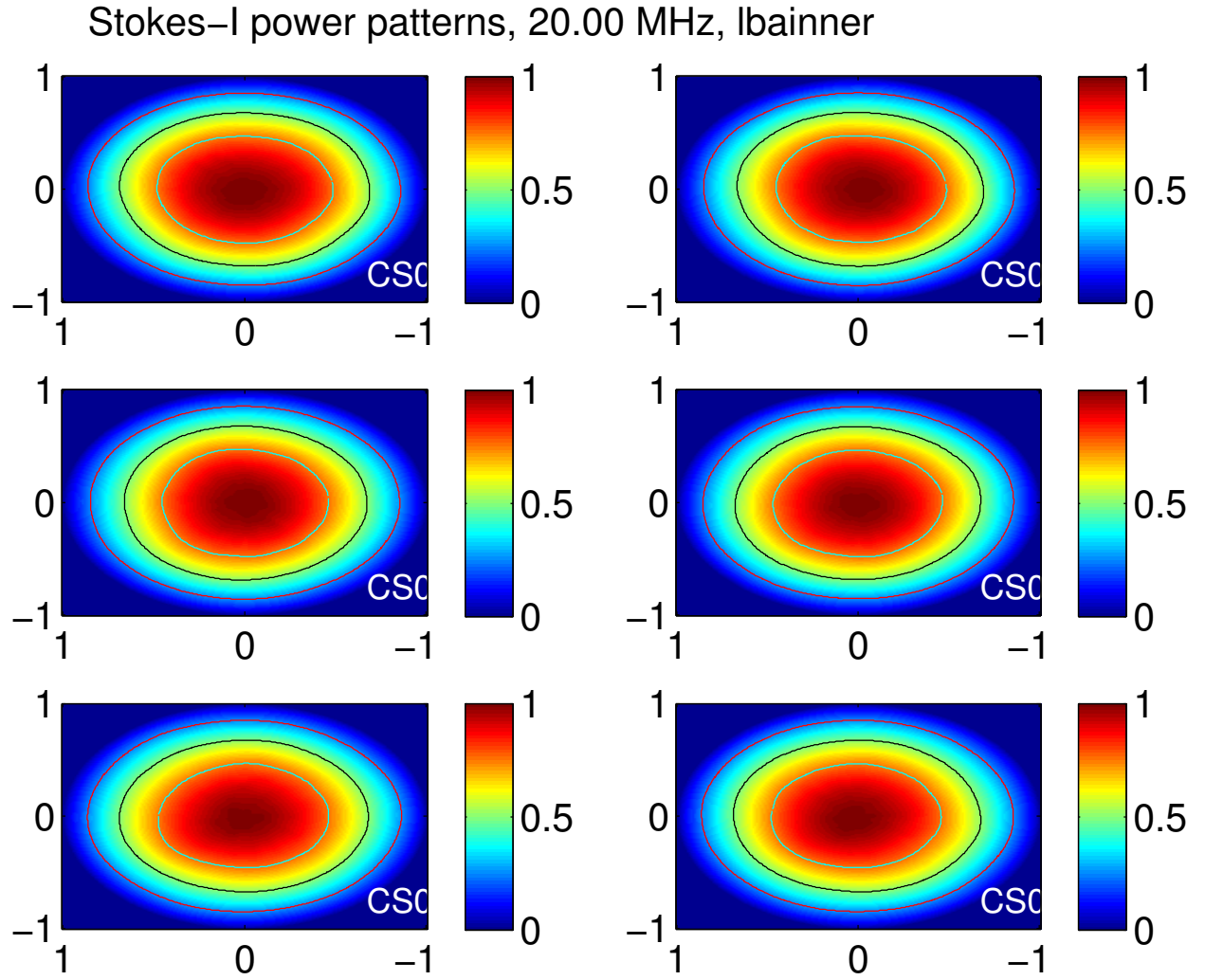


Figure 13: Stokes-I beam shapes from superterp stations for LBA INNER configuration, 20MHz.

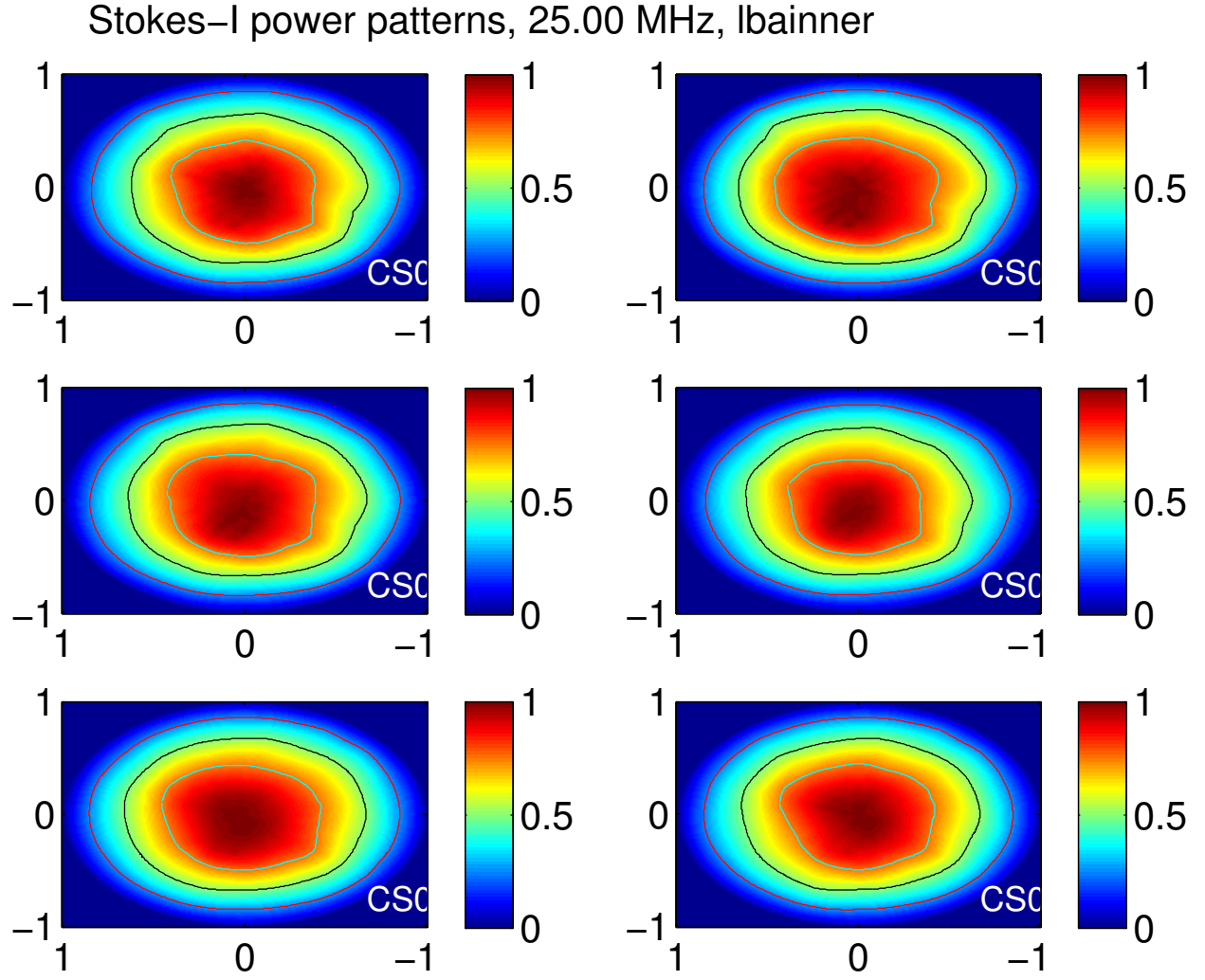


Figure 14: Stokes-I beam shapes from superterp stations for LBA INNER configuration, 25MHz.

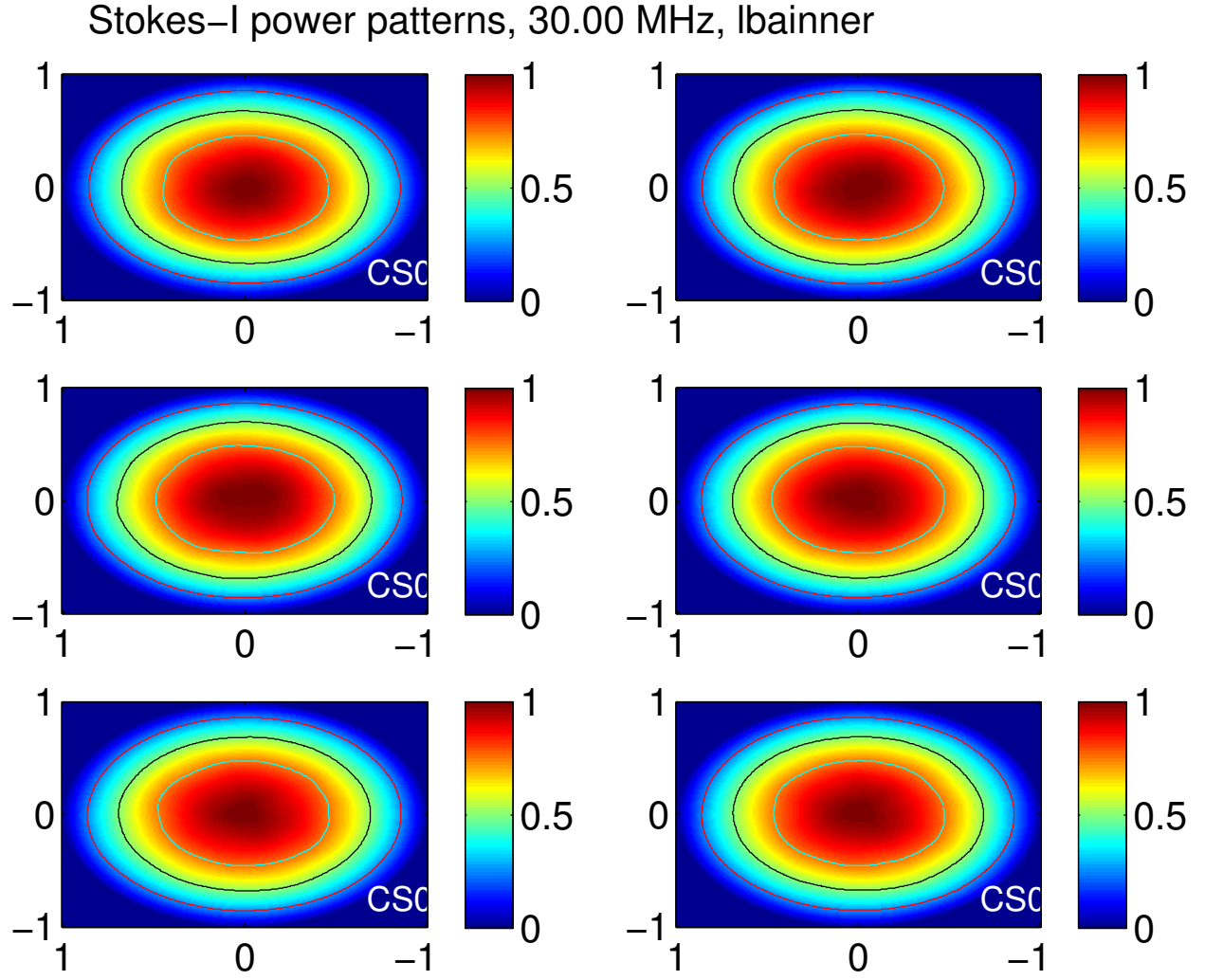


Figure 15: Stokes-I beam shapes from superterp stations for LBA INNER configuration, 30MHz.

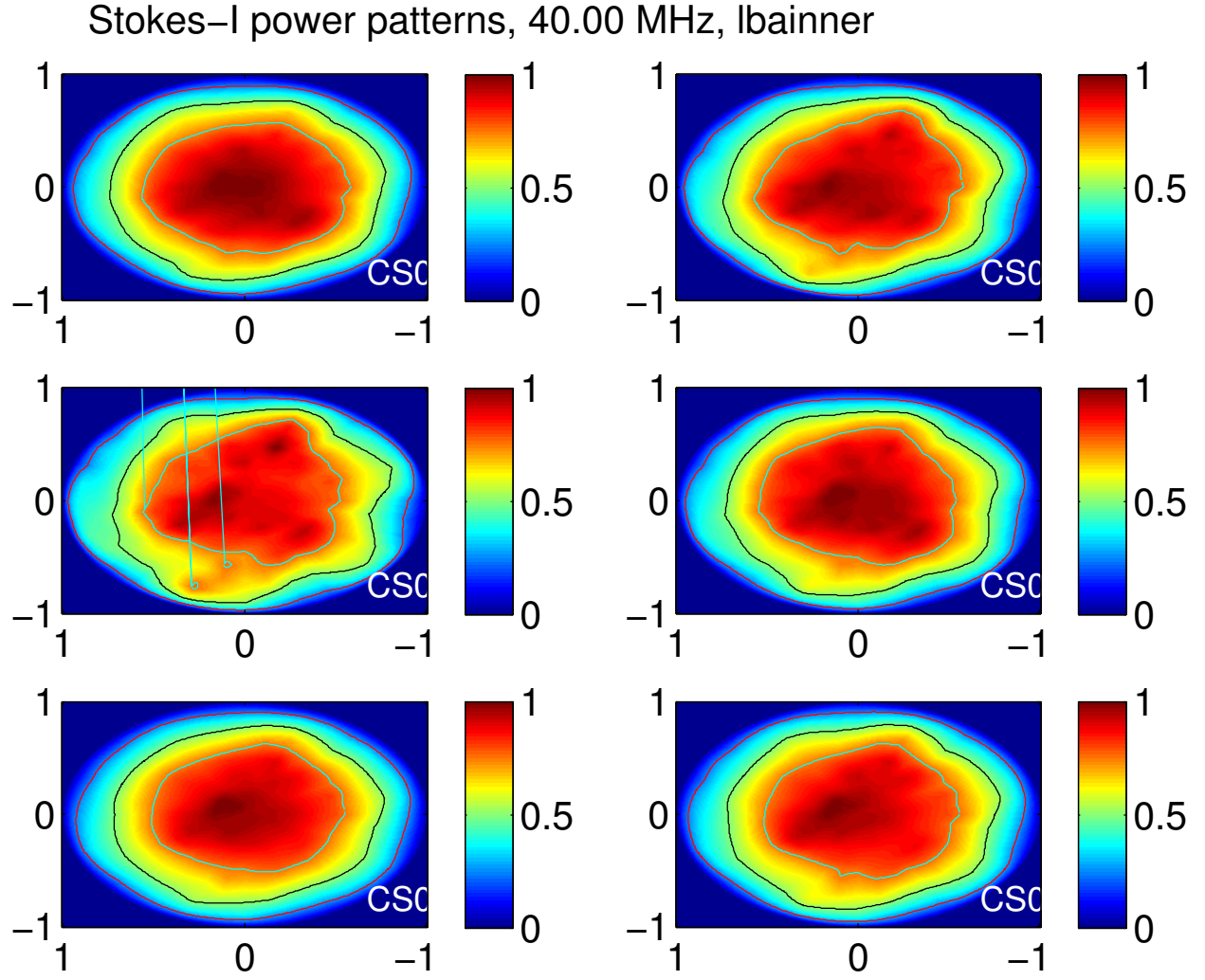


Figure 16: Stokes-I beam shapes from superterp stations for LBA INNER configuration, 40MHz.

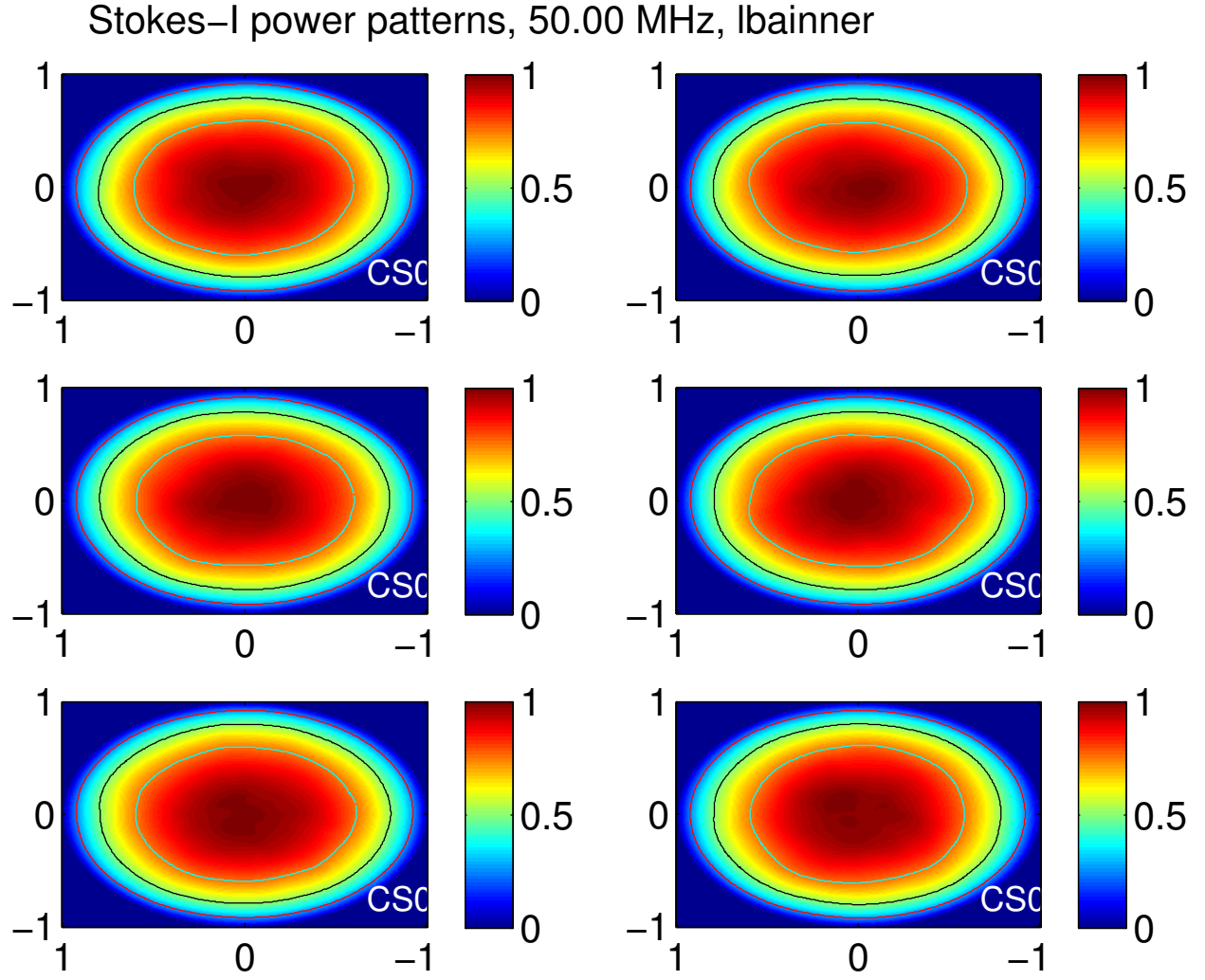


Figure 17: Stokes-I beam shapes from superterp stations for LBA INNER configuration, 50MHz.

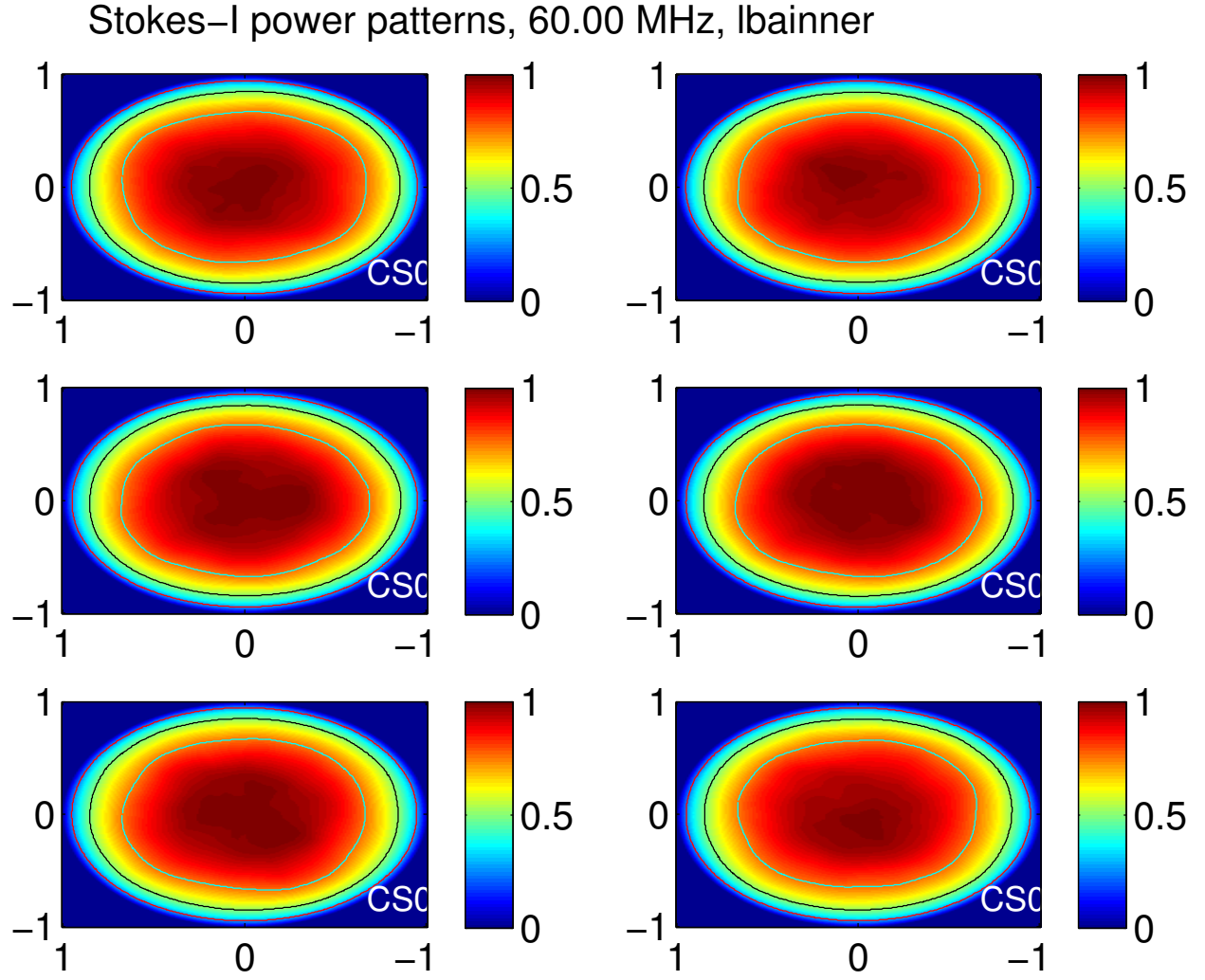


Figure 18: Stokes-I beam shapes from superterp stations for LBA INNER configuration, 60MHz.

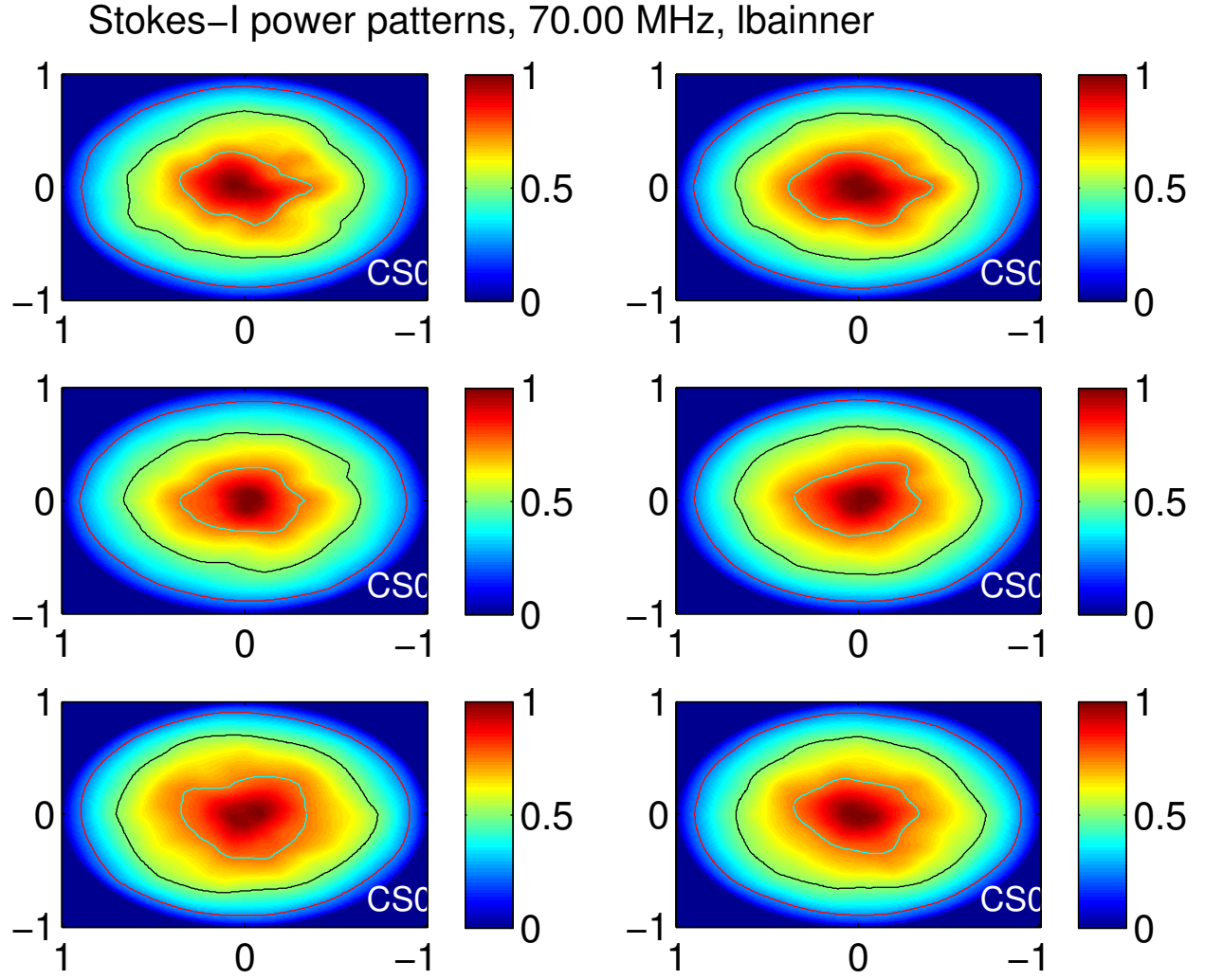


Figure 19: Stokes-I beam shapes from superterp stations for LBA INNER configuration, 70MHz.

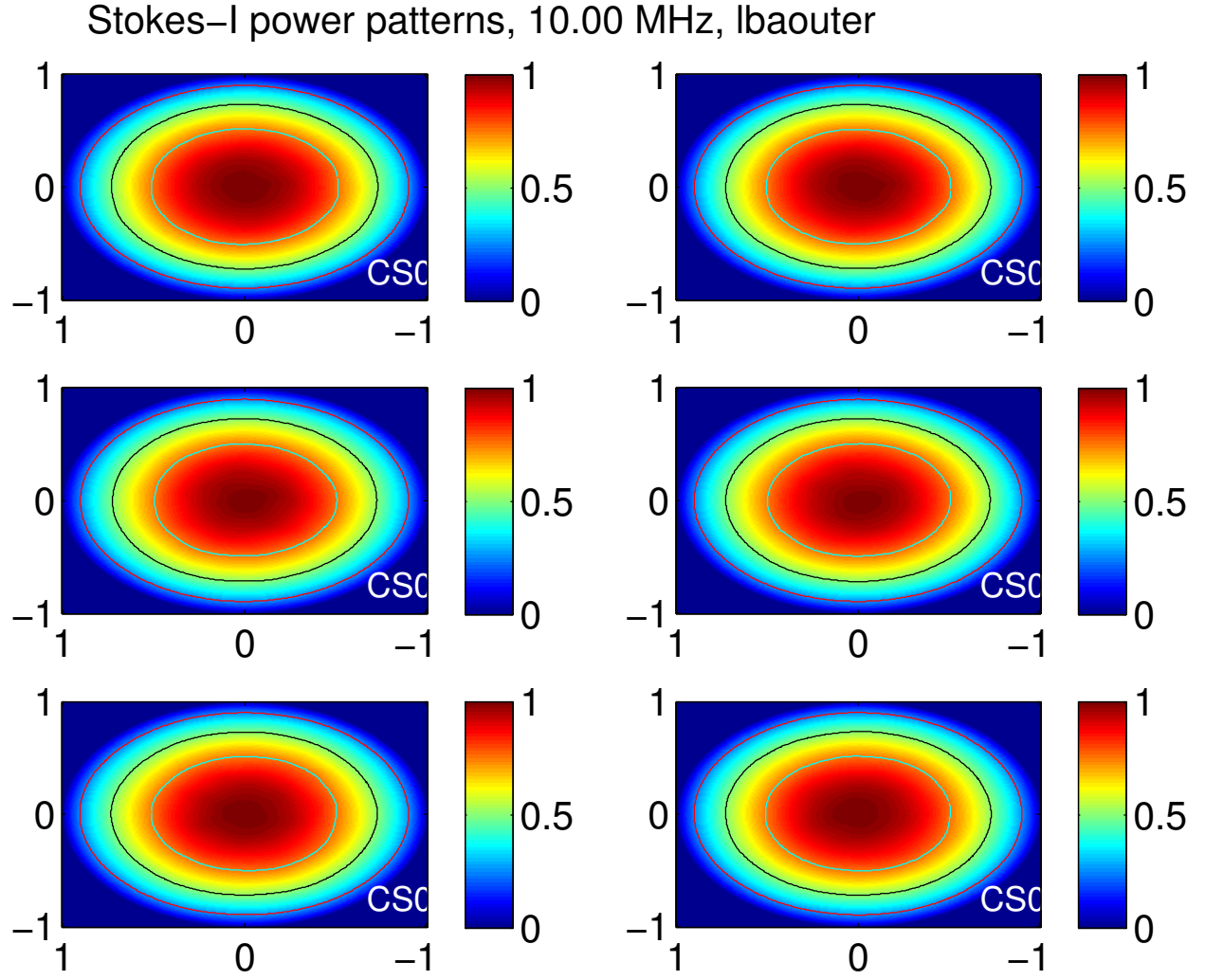


Figure 20: Stokes-I beam shapes from superterp stations for LBA-OUTER configuration, 10MHz.

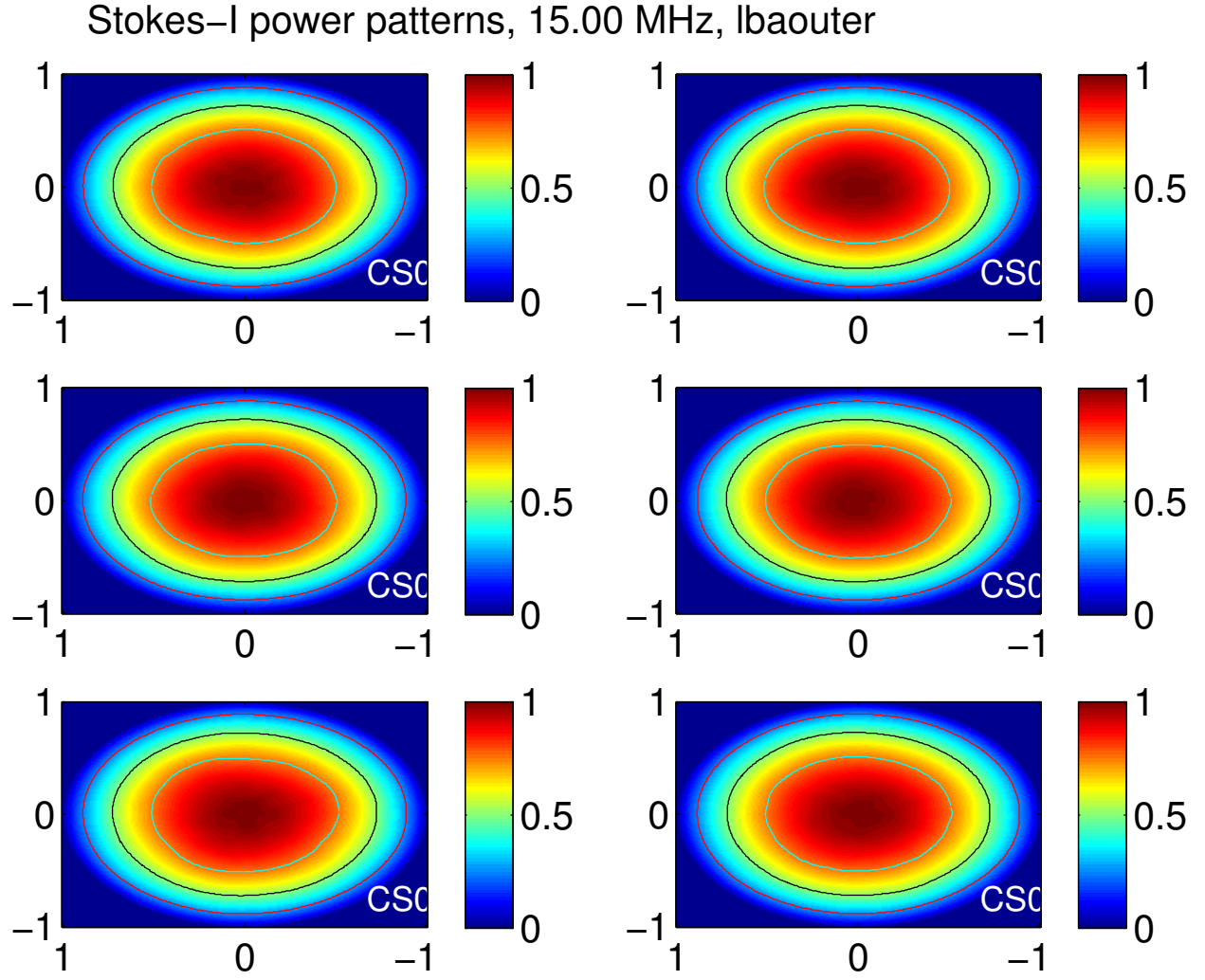


Figure 21: Stokes-I beam shapes from superterp stations for LBA_OUTER configuration, 15MHz.

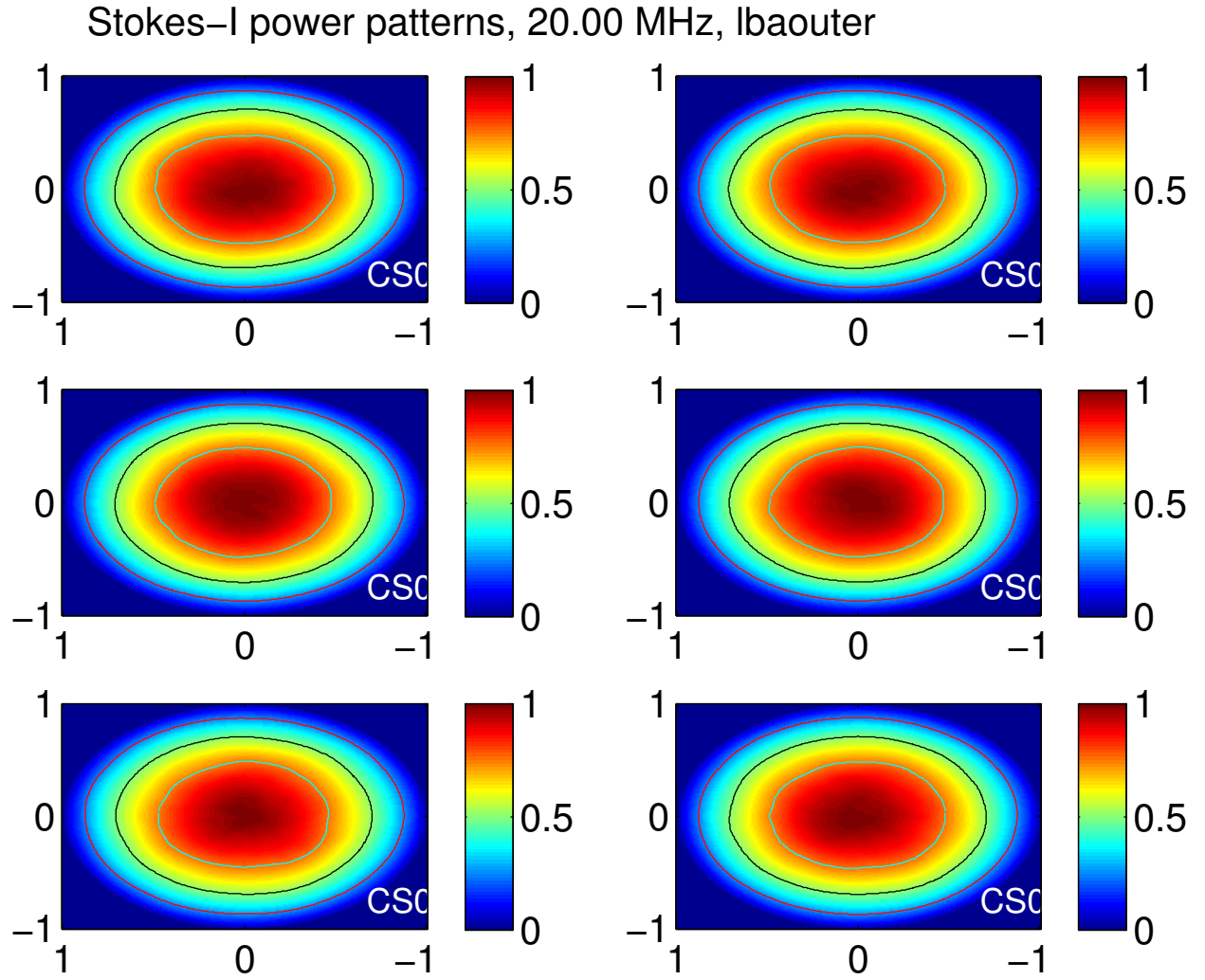


Figure 22: Stokes-I beam shapes from superterp stations for LBA_OUTER configuration, 20MHz.

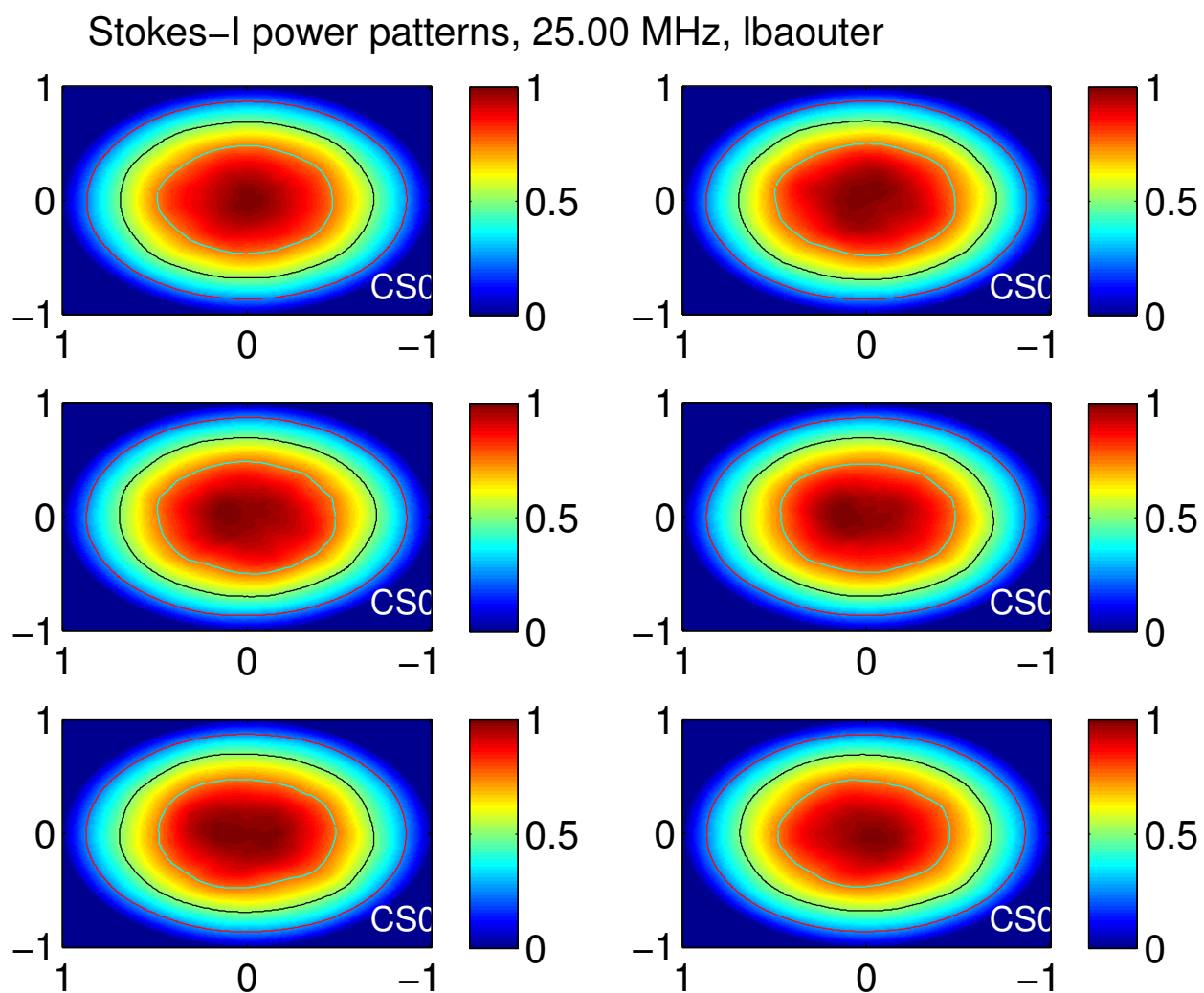


Figure 23: Stokes-I beam shapes from superterp stations for LBA_OUTER configuration, 25MHz.

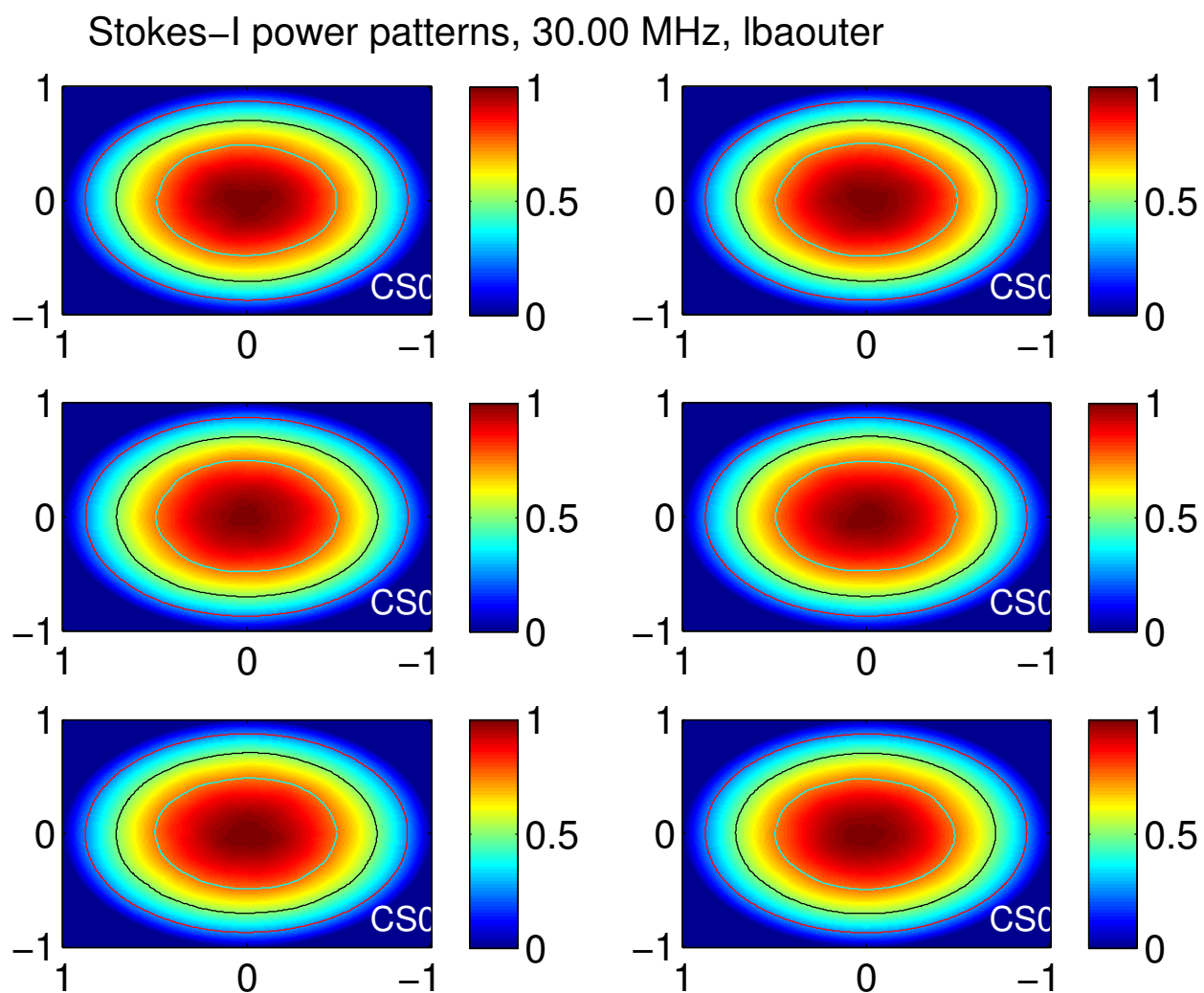


Figure 24: Stokes-I beam shapes from superterp stations for LBA_OUTER configuration, 30MHz.

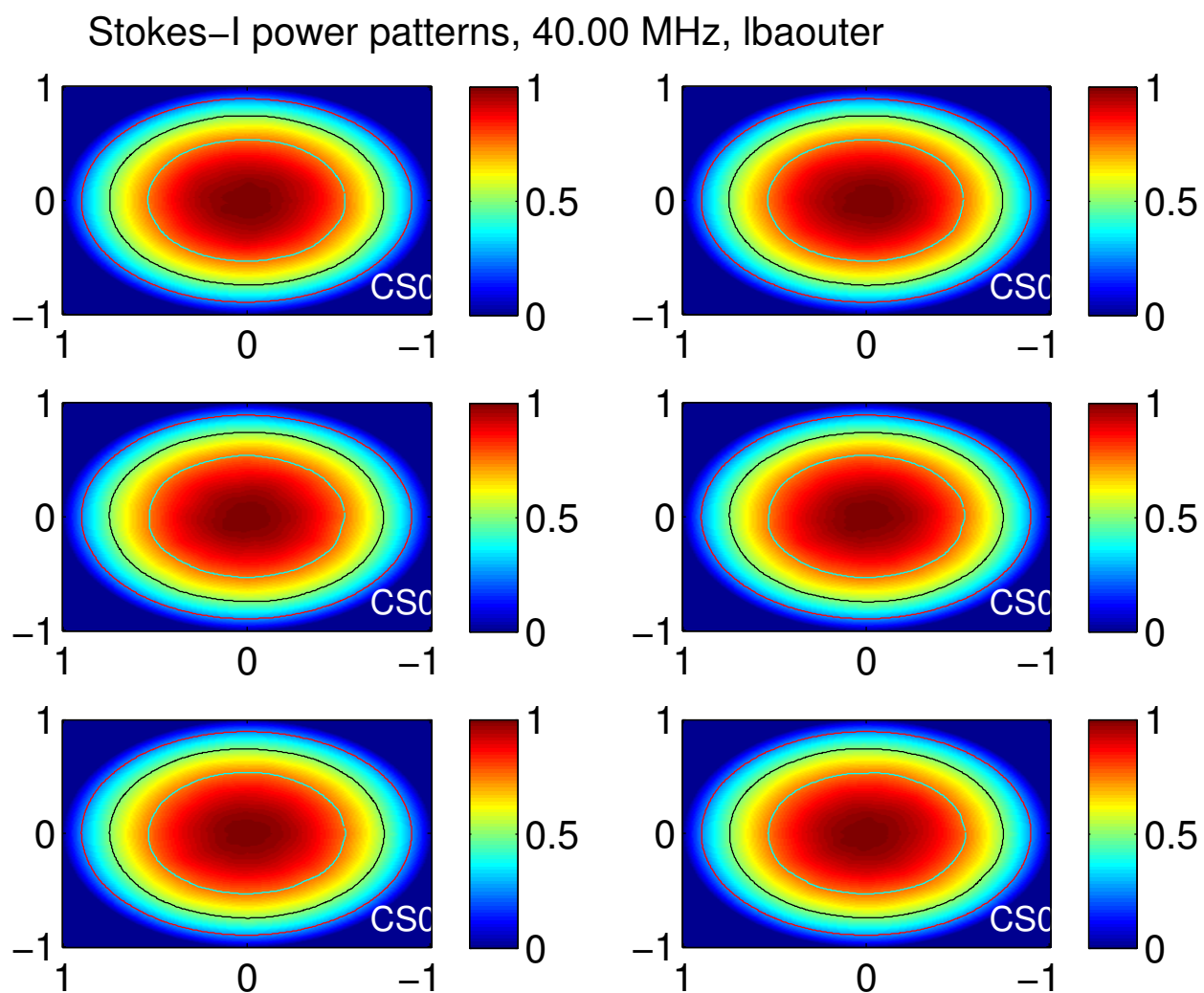


Figure 25: Stokes-I beam shapes from superterp stations for LBA_OUTER configuration, 40MHz.

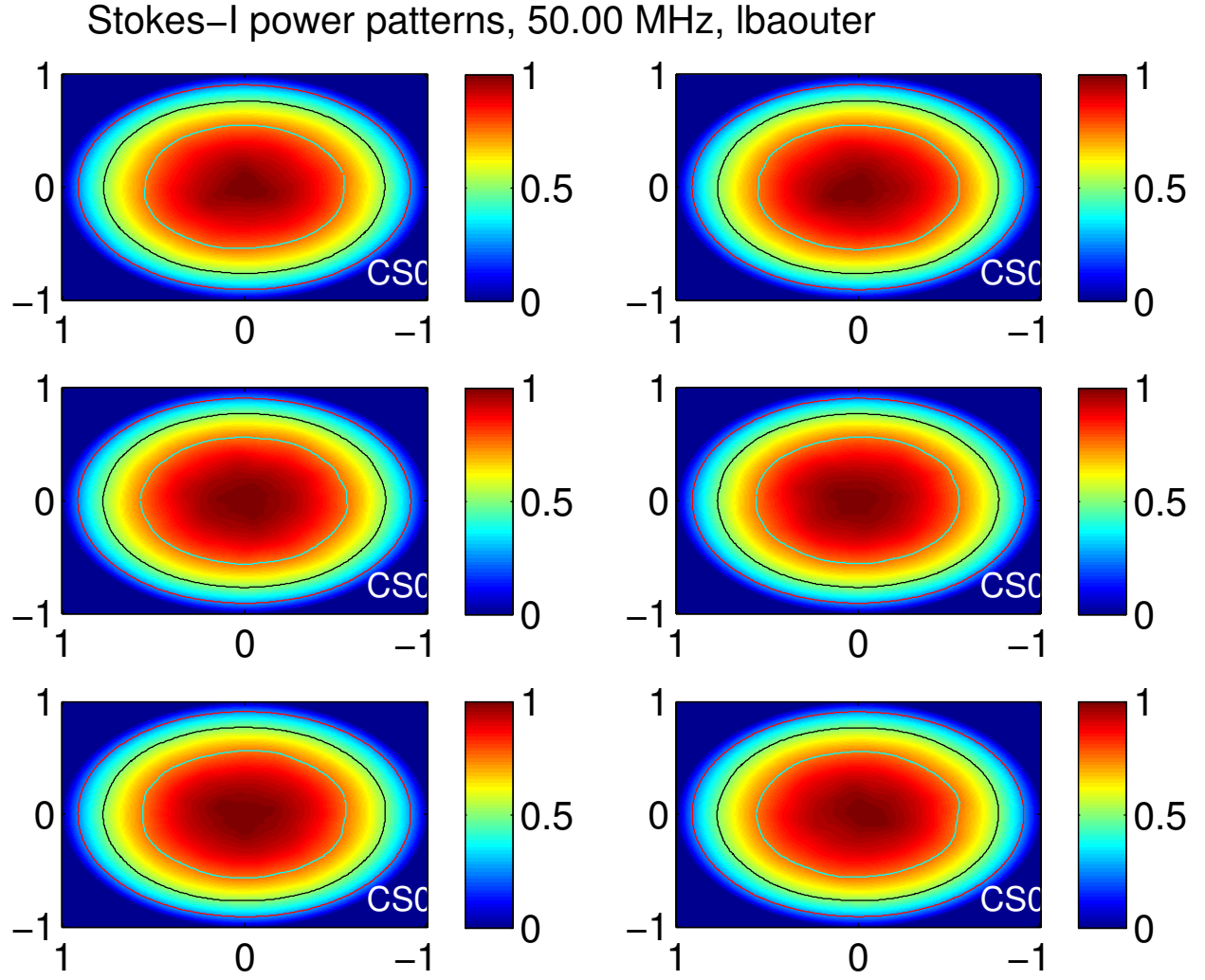


Figure 26: Stokes-I beam shapes from superterp stations for LBA_OUTER configuration, 50MHz.

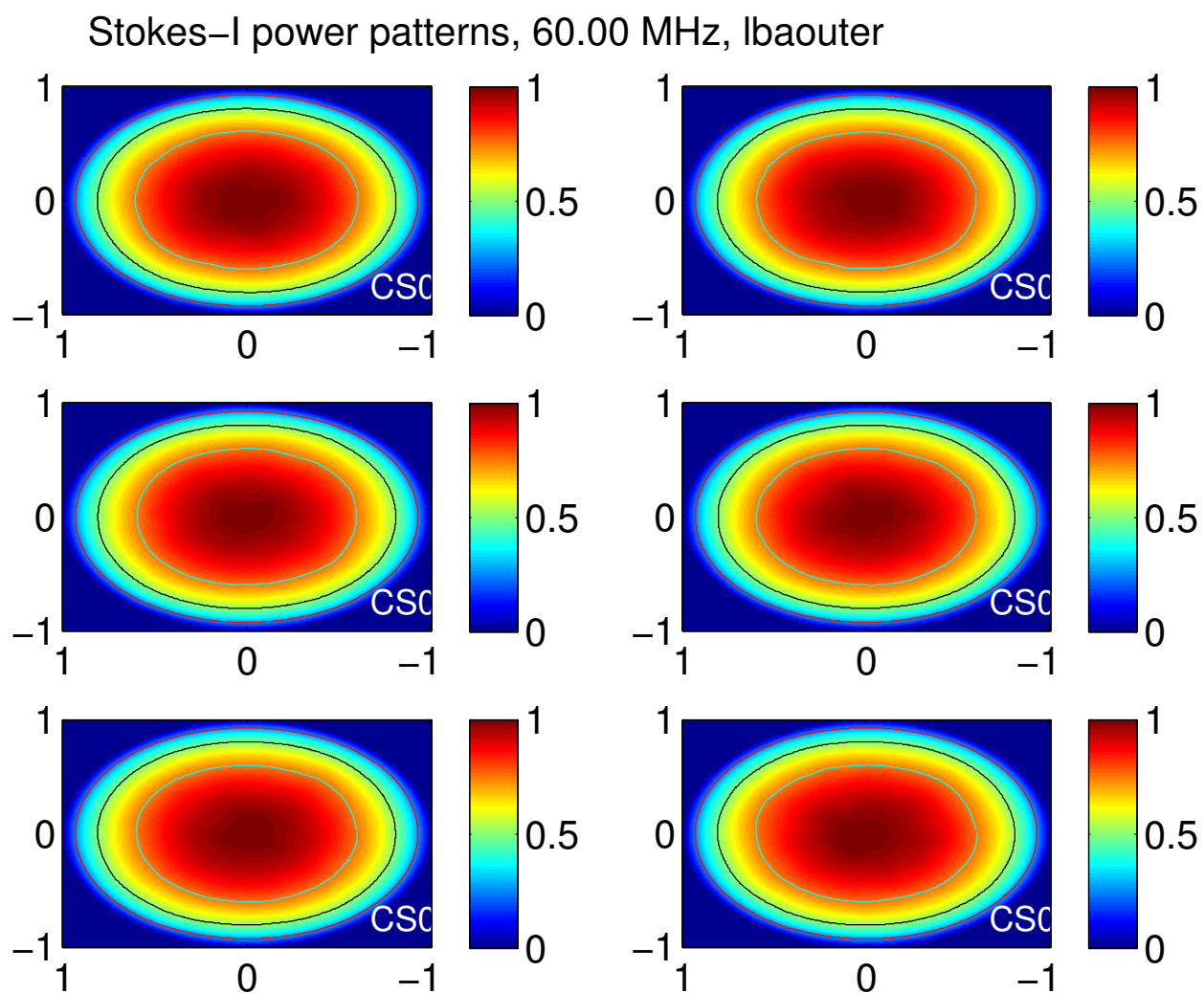


Figure 27: Stokes-I beam shapes from superterp stations for LBA_OUTER configuration, 60MHz.

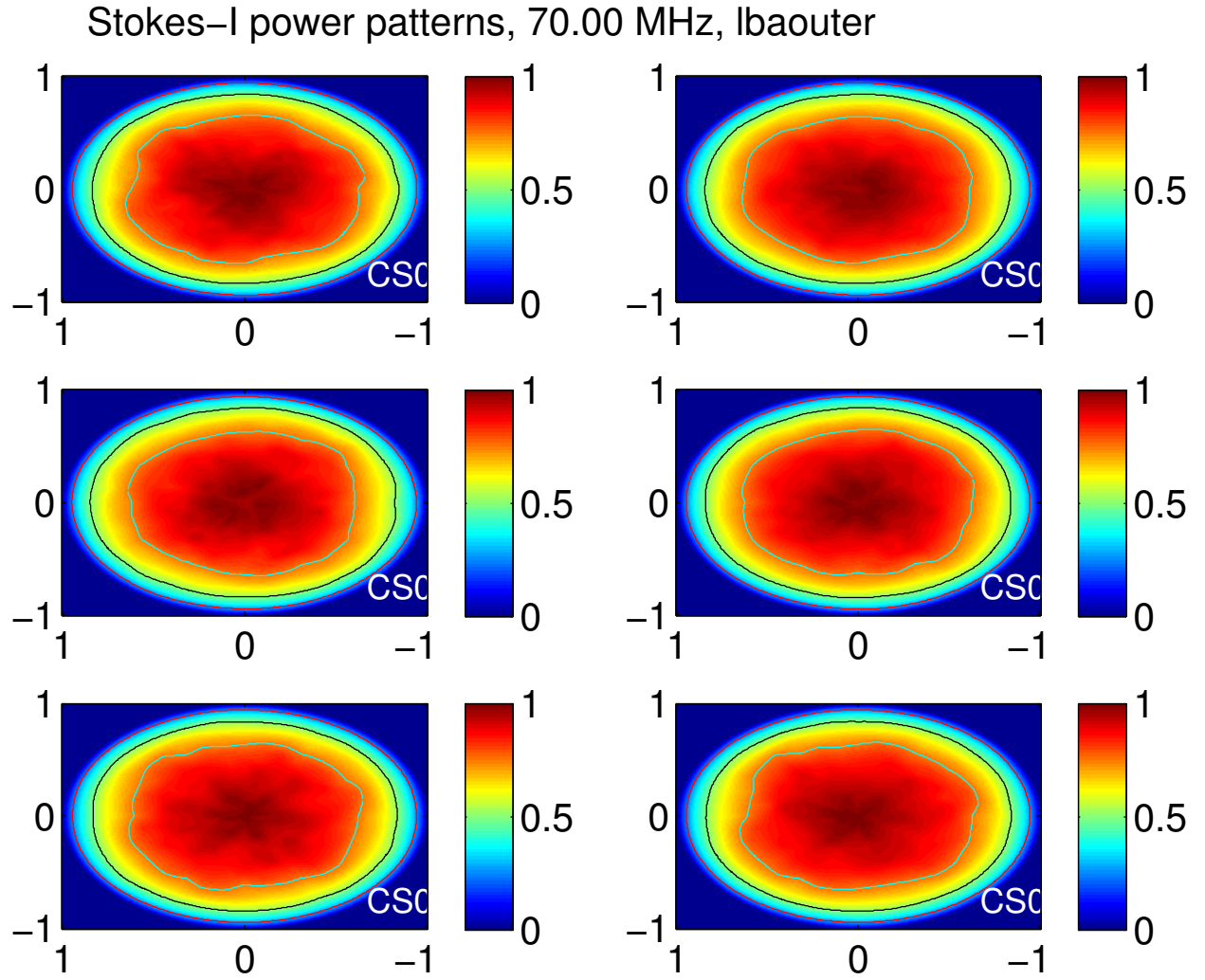


Figure 28: Stokes-I beam shapes from superterp stations for LBA_OUTER configuration, 70MHz.